

Semi-supervised Neural Chord Estimation Based on a Variational Autoencoder with Latent Chord Labels and Features

Yiming Wu, Tristan Carsault, Eita Nakamura, Kazuyoshi Yoshii, *Member, IEEE*

Abstract—This paper describes a statistically-principled semi-supervised method of automatic chord estimation (ACE) that can make effective use of music signals regardless of the availability of chord annotations. The typical approach to ACE is to train a deep *classification* model (neural chord estimator) in a supervised manner by using only annotated music signals. In this *discriminative* approach, prior knowledge about chord label sequences (model output) has scarcely been taken into account. In contrast, we propose a unified *generative* and *discriminative* approach in the framework of amortized variational inference. More specifically, we formulate a deep *generative* model that represents the generative process of chroma vectors (observed variables) from discrete labels and continuous features (latent variables), which are assumed to follow a Markov model favoring self-transitions and a standard Gaussian distribution, respectively. Given chroma vectors as observed data, the posterior distributions of the latent labels and features are computed approximately by using deep *classification* and *recognition* models, respectively. These three models form a variational autoencoder and can be trained jointly in a semi-supervised manner. The experimental results show that the regularization of the classification model based on the Markov prior of chord labels and the generative model of chroma vectors improved the performance of ACE even under the supervised condition. The semi-supervised learning using additional non-annotated data can further improve the performance.

Index Terms—Automatic chord estimation, semi-supervised learning, variational autoencoder.

I. INTRODUCTION

A Chord is a mid-level representation of polyphonic music that lies between the highly-abstracted musical intentions of humans and actual musical sounds. Unlike musical notes, chord sequences do not tell the actual pitches, but abstractly represent the harmonic content evolving over time. In lead sheets (a form of music notation consisting of melody, chords, and lyrics), chord labels are shown to musicians to roughly suggest the intentions of how musical notes should be arranged and played in each bar.

Manuscript received March 18, 2020; revised XXXX XX, 2020; accepted XXXX XX, 2020; Date of publication XXXX XX, 2020; date of current version XXXX XX, 2020. This work was supported by JST ACCEL No. JP-MJAC1602 and JSPS KAKENHI Nos. 19H04137, 19K20340, and 16H01744. The associate editor coordinating the review of this manuscript and approving it for publication is XXX XXX. (*Corresponding author: Yiming Wu.*)

Y. Wu, E. Nakamura, and K. Yoshii are with Graduate School of Informatics, Kyoto University, Kyoto 606-8501, Japan (email: {wu, enakamura, yoshii}@sap.ist.i.kyoto-u.ac.jp). E. Nakamura is also with Hakubi Center for Advanced Research, Kyoto University, Kyoto 606-8501, Japan.

T. Carsault is with Représentations Musicales, IRCAM, 75004 Paris, France (email: tristan.carsault@ircam.fr).

Digital Object Identifier 10.1109/TASLP.2020.XXXXXXX

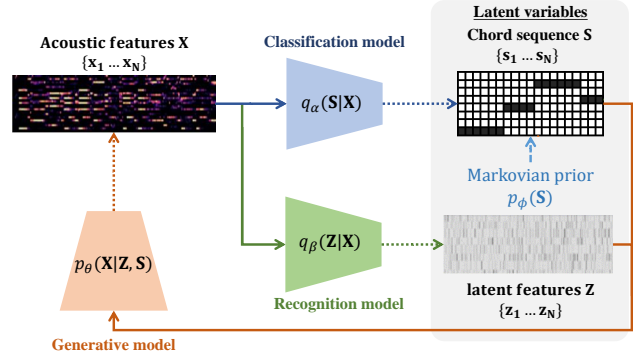


Fig. 1. The proposed variational autoencoder consisting of a deep generative model of chroma vectors, a deep classification model of chord labels, and a deep recognition model of latent features. Dashed arrows indicate stochastic relations. These three models are trained jointly in a semi-supervised manner by using annotated and non-annotated music signals.

Automatic chord estimation (ACE), which aims to recognize the chord sequence behind a music signal, has been one of the fundamental research topics in the field of music information retrieval (MIR). For example, it forms the basis of music content visualization (*e.g.*, Songle [1]), and higher-level MIR tasks such as genre classification [2] and cover song retrieval [3]. The diversity and complexity of the acoustic characteristics of music signals make the ACE task very challenging. ACE studies have thus been focusing on data-driven methods based on statistical models [4], which are roughly categorized into *generative* and *discriminative* approaches.

Early studies took the *generative* approach based on a classical probabilistic latent variable model. For example, a hidden Markov model (HMM) is often used to represent the stochastic generative process of chroma vectors (observed variables) from chord labels (latent variables) [5]. Given chroma vectors, the chord labels are inferred such that their likelihood is maximized. An advantage of this approach is that the prior distribution of chord labels (language model) can be naturally introduced. To encourage the estimated chord labels to be consistent with musical grammar, the temporal continuity and dynamics of chord labels should be considered. Another advantage is that in theory generative models can be trained in a semi-supervised or even unsupervised manner. However, the expressive power of simple generative models like HMMs have been insufficient to represent the temporal structure of chord labels and the relationships between acoustic features and chord labels.

The *discriminative* approach, in contrast, aims to directly

convert acoustic features into chord labels. Recently, deep neural networks (DNNs) have often been used for estimating the posterior probabilities of chord labels. Because the generative process is not considered explicitly, the oversimplified assumptions posed by the generative approach can be avoided [6], and chord label inference is more straightforward. A problem here is that the classifier is usually trained for learning a frame-level audio-to-label mapping without considering the characteristics of chord label sequences and the generative process of music. In addition, the model needs to be trained in a fully-supervised manner. Manual chord annotation is a labor-intensive task, and the performance of ACE heavily depends on the amount, diversity and quality of annotated music signals [7] because of the nature of supervised learning.

Given that the performance of ACE could be improved by integrating the complementary generative and discriminative approaches, we propose a semi-supervised neural chord estimator based on a variational autoencoder (VAE) [8] (Fig. 1). Because chroma vectors can be represented more precisely by considering their continuous latent features (deviations from basic chroma patterns) in addition to the underlying discrete chord labels, we formulate a DNN-based *generative* model p_θ that represents the generative process of a sequence of chroma vectors from that of chord labels and that of latent features. To complete the Bayesian formulation, we introduce prior distributions on the latent variables. Specifically, the chord labels are assumed to follow a first-order Markov model favoring self transitions, and the latent features, which abstractly represent the fine structure of the chroma vectors, are assumed to follow a standard Gaussian distribution. In the framework of amortized variational inference (AVI) [9], DNN-based *discriminative* models q_α and q_β are then introduced as variational posterior distributions to approximate the posterior distribution of the latent variables from an observed chroma sequence. The generative and discriminative models can be trained jointly in a semi-supervised manner by using music signals with and without chord annotations.

The main contribution of this paper is to draw the potential of the powerful deep discriminative model for ACE, by integrating it into the principled statistical inference formalism of the generative approach. This is the first attempt to use a VAE for semi-supervised ACE. A key feature of our VAE is that a Markov model is used to define the prior probability of chord label sequences, which works as a chord language model and prevents frequent frame-level transitions of chord labels in the joint training of the generative and discriminative models for given chroma vectors. We experimentally show the effectiveness of this regularization on semi-supervised learning.

The remainder of this paper is organized as follows. Section II reviews related work on the generative and discriminative approaches to ACE. Section III describes the proposed ACE method based on the semi-supervised VAE with the Markov prior on latent chord labels. Section IV reports the experimental results and discusses the effectiveness and limitations of the proposed techniques. Section V summarizes the paper.

II. RELATED WORK

This section reviews related work on ACE based on generative and discriminative approach, and machine-learning strategies for integrating these approaches.

A. Generative Approach

In the generative approach, a probabilistic generative model $p(\mathbf{X}, \mathbf{S}) = p(\mathbf{X}|\mathbf{S})p(\mathbf{S})$ has often been formulated as an HMM [10], where \mathbf{X} and \mathbf{S} denote a sequence of acoustic features (e.g., chroma vectors [11]) and a sequence of chord labels [12], respectively. The emission probabilities of \mathbf{X} for each chord, $p(\mathbf{X}|\mathbf{S})$, and the chord transition probabilities, $p(\mathbf{S})$, are typically given by a Gaussian mixture model (GMM) and a first-order or higher-order Markov model (n-gram model), respectively. Given \mathbf{X} as observed data, the optimal chord label sequence maximizing the posterior probability $p(\mathbf{S}|\mathbf{X})$ can be estimated efficiently by using the Viterbi algorithm.

Many HMM-based methods have been proposed for ACE. Lee and Slaney [5], for example, proposed joint training of multiple HMMs corresponding to different keys. Another research direction is to simultaneously deal with multiple kinds of musical elements in addition to chord labels by explicitly considering the relationships of those elements. Mauch and Dixon [13] proposed a dynamic Bayesian network (DBN) that represents the hierarchical structure over metrical positions, musical keys, bass notes, and chords, and formulates the generative process of treble and bass chroma vectors. Similarly, Ni *et al.* [14] proposed a harmony progression analyzer (HPA) based on a DBN whose latent states represent chords, inversions, and musical keys.

Some studies have focused on the temporal characteristics of frame-level chord labels. To represent repetitions of chord patterns, for example, multi-order HMMs [15] and duration-explicit HMMs [16] have been proposed, where the results of ACE were found to be insensitive to the frame-level transition probabilities of chord labels [16]. Although such a frame-level language model is incapable of learning typical chord progressions at the symbol level, it is still effective for encouraging the continuity of chord labels at the frame level.

B. Discriminative Approach

Recently, DNNs have intensively been used as a powerful discriminative model for directly estimating the posterior probability $p(\mathbf{S}|\mathbf{X})$. Humphrey and Bello [17], for example, used a convolutional neural network (CNN) for learning an effective representation of raw audio spectrograms. A number of ACE methods using DNN classifiers have then been proposed for using low-level audio representations such as constant-Q transform (CQT) spectrograms [18]. In general, these DNN-based methods outperform HMM-based generative methods [19].

Because typical DNN-based methods estimate the posterior probabilities of chord labels at the frame level, some smoothing technique is often used for estimating temporally-coherent chord labels. An HMM [20] or a conditional random field (CRF) [19], for example, can be used for estimating the optimal path of chord labels from the estimated posterior

probabilities. Recurrent neural networks (RNNs) have recently been used as a language model that represents the long-term dependency of chord labels [21], [22]. Note that RNN-based models are still incapable of learning the symbol-level syntactic structure from frame-level chord sequences [23]. To solve this problem, Korzeniowski and Widmer [24] formulated a symbol-level chord transition model with a duration distribution. Chen and Su [25] proposed an extension of the transformer model [26] for joint chord segmentation and labeling in a context of multi-task learning.

Even the state-of-the-art neural chord estimators have difficulty in identifying infrequent chord types because the numbers of occurrences of chord types are highly imbalanced. In fact, the majority of chords is occupied by major and minor triads. Another difficulty lies in distinguishing chords that commonly include several pitch classes as chord notes (*e.g.*, C9 and Csus2). When the chord vocabulary gets larger, *i.e.*, the chord classes are defined at a finer level, the subjectivity of annotators leads to the inconsistency of chord annotations [27]. This would make infrequent chord types harder to learn. This problem can be mitigated by reflecting the musical knowledge about the constituent tones and taxonomy of chord labels [28]–[30] into objective functions and/or by using an even-chance training scheme [31]. However, dealing with a large chord vocabulary is still an open problem.

C. Unified Generative and Discriminative Approach

Integration of deep generative and discriminative models has actively been explored in the context of unsupervised or semi-supervised learning. One of the most popular strategies is to use a variational autoencoder (VAE) [8] that jointly optimizes a deep generative model $p(\mathbf{X}|\mathbf{S})$ and a deep recognition model $q(\mathbf{S}|\mathbf{X})$ that approximates $p(\mathbf{S}|\mathbf{X})$ such that the lower bound of the marginal likelihood $p(\mathbf{X})$ is maximized. An extension, known as conditional VAE [32], can be used for semi-supervised learning of latent representations disentangled from given labels (conditions) [33]. In the field of Automatic Speech Recognition (ASR), some studies tried to jointly train a speech-to-text model with a text-to-speech model to improve the performance of ASR by using both annotated and non-annotated speech signals [34].

In this paper, we use a VAE with two different latent variables corresponding to chord labels (*categorical* variables) and latent features (*continuous* variables). This model is similar to JointVAE [35] in a sense that both discrete and continuous representations are learned jointly. In our model, a Markov prior favoring self transitions is put on chord labels for regularizing the recognition model in the VAE training. In conventional studies, in contrast, the Markov prior is used only for smoothing chord labels estimated by a recognition model. To our knowledge, our work is the first attempt to integrate the generative and discriminative processes between chord labels and acoustic features into a unified jointly-trainable DNN.

III. PROPOSED METHOD

This section describes the proposed unified generative and discriminative approach to ACE (Fig. 2). To tackle the frame-level ACE (Section III-A), we formulate a probabilistic model

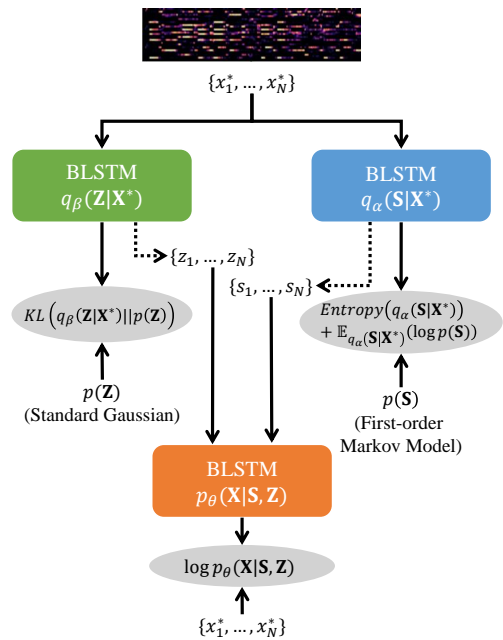


Fig. 2. The computation flow of the unsupervised learning. The gray areas correspond to the four terms of the cost function $\mathcal{L}_{\mathbf{X}}$ given by (10).

p_θ representing the generative process of chroma vectors from chord labels and latent features (Section III-B), and then introduce neural statistical estimators q_α and q_β that respectively infers chord labels and latent features from chroma vectors (Section III-C). These three models are jointly trained in the framework of amortized variational inference (AVI) [9]. In theory, q_α can be trained in an unsupervised manner only from chroma vectors without referring to their chord labels (Section III-D). In practice, q_α is trained in a supervised or semi-supervised manner by using paired data (Sections III-E).

A. Problem Specification

For simplified explanation, suppose that we have one musical piece. Let $\mathbf{X} = \{\mathbf{x}_1, \dots, \mathbf{x}_N\}$ be a sequence of chroma vectors extracted from the music signal, where $\mathbf{x}_n \in \{0, 1\}^D$ is a D -dimensional binary vector representing the activations of D pitch classes at frame n , and N is the number of frames. In this paper, \mathbf{x}_n is a 3-channel chroma vector, each channel representing the lower, middle, and higher pitch ranges respectively ($D = 12 \times 3 = 36$), as defined in [36]. Because the true pitch activations are not given in reality, \mathbf{x}_n is obtained by using a neural multi-pitch estimator [36] that estimates frame-wise pitch-class distributions with a DNN trained from 6,000 pieces (audio signals synthesized from MIDI files)¹. We thus relax the binary constraint and assume $\mathbf{x}_n \in [0, 1]^D$.

Let $\mathbf{S} = \{\mathbf{s}_1, \dots, \mathbf{s}_N\}$ be a sequence of chord labels corresponding to \mathbf{X} , where $\mathbf{s}_n \in \{0, 1\}^K$ is a categorical variable (K -dimensional one-hot vector) indicating the chord label of frame n . In this paper, the chord vocabulary consists of all possible combinations of twelve root notes with six types of triad chords (with shorthands *maj*, *min*, *dim*, *aug*, *sus2*, and *sus4*) and two types of power chords (with shorthands *1* and *5*), and

¹ <https://github.com/Xiao-Ming/ChordRecognitionMIDITrainedExtractor>

a no-chord label (with shorthand N), *i.e.*, $K = 12 \times 8 + 1 = 97$. We follow Harte's notation [37], *e.g.*, C:maj and C#:sus4.

Let $\mathbf{Z} = \{\mathbf{z}_1, \dots, \mathbf{z}_N\}$ be a sequence of latent features, where $\mathbf{z}_n \in \mathbb{R}^L$ is a continuous variable that abstractly represents how \mathbf{x}_n is deviated from a basic chroma pattern specified by \mathbf{s}_n ($L = 64$). *i.e.*, not only \mathbf{s}_n but also \mathbf{z}_n are needed to fully describe \mathbf{x}_n . If a region of C:maj includes some passing notes with different volumes, for example, the chroma vectors are deviated from a basic pattern that takes one at the dimensions corresponding to C, E, and G.

Our goal is to train a classification model $p(\mathbf{S}|\mathbf{X})$ and use it for estimating chord labels behind unseen music signals. In an unsupervised condition, the classification model should be trained from \mathbf{X} without using the ground-truth data of \mathbf{S} . In a supervised condition, the classification model can be trained by using paired data of \mathbf{X} and \mathbf{S} . In a semi-supervised condition, some part of \mathbf{S} is given as ground-truth data.

B. Generative Model

We formulate a probabilistic hierarchical generative model (joint probability distribution) of chord labels \mathbf{S} , latent features \mathbf{Z} , and chroma vectors \mathbf{X} as follows:

$$p_{\theta, \phi}(\mathbf{X}, \mathbf{S}, \mathbf{Z}) = p_{\theta}(\mathbf{X}|\mathbf{S}, \mathbf{Z})p_{\phi}(\mathbf{S})p(\mathbf{Z}), \quad (1)$$

where $p_{\theta}(\mathbf{X}|\mathbf{S}, \mathbf{Z})$ is a likelihood function of \mathbf{S} and \mathbf{Z} for \mathbf{X} , $p_{\phi}(\mathbf{S})$ is a prior distribution of \mathbf{S} , $p(\mathbf{Z})$ is the prior of \mathbf{Z} , and θ and ϕ are model parameters. While standard HMMs used for ACE are represented as $p_{\theta, \phi}(\mathbf{X}, \mathbf{S}) = p_{\theta}(\mathbf{X}|\mathbf{S})p_{\phi}(\mathbf{S})$ [6], we use both \mathbf{S} and \mathbf{Z} for precisely representing \mathbf{X} , *i.e.*, $p_{\theta}(\mathbf{X}|\mathbf{S}, \mathbf{Z})$ is a deep *generative* model represented as follows:

$$p_{\theta}(\mathbf{X}|\mathbf{S}, \mathbf{Z}) = \prod_{n=1}^N \prod_{d=1}^D \text{Bernoulli}(x_{nd} | [\omega_{\theta}(\mathbf{S}, \mathbf{Z})]_{nd}), \quad (2)$$

where $\omega_{\theta}(\mathbf{S}, \mathbf{Z})$ is the ND -dimensional output of a DNN with parameters θ that takes \mathbf{S} and \mathbf{Z} as input and the notation $[\mathbf{A}]_{ij}$ indicates the ij -th element of \mathbf{A} . Although x_{nd} should take a binary value in theory, we allow it to take a real value between 0 and 1 from a practical point of view.

If we have no prior knowledge on chord labels \mathbf{S} , a natural choice of $p_{\phi}(\mathbf{S})$ is a uniform distribution as follows:

$$p_{\phi}(\mathbf{S}) = \prod_{n=1}^N \text{Categorical}(\mathbf{s}_n | [\frac{1}{K}, \dots, \frac{1}{K}]), \quad (3)$$

Since chord labels \mathbf{S} have temporal continuity, *i.e.*, change infrequently at the frame level, we follow the common assumption on chord labels [12] and use a first-order Markov model favoring self-transitions of chord labels as the chord label prior $p_{\phi}(\mathbf{S})$ as follows:

$$\begin{aligned} p_{\phi}(\mathbf{S}) &= p(\mathbf{s}_1) \prod_{n=2}^N p(\mathbf{s}_n | \mathbf{s}_{n-1}) \\ &= \prod_{k=1}^K \phi_k^{s_{1k}} \prod_{n=2}^N \prod_{k'=1}^K \prod_{k=1}^K \phi_{k'k}^{s_{n-1, k'} s_{nk}}, \end{aligned} \quad (4)$$

where ϕ_k is the initial probability of chord k and $\phi_{k'k}$ is the transition probability from chord k' to chord k . Since ϕ_k and

$\phi_{k'k}$ represent the probabilities, $\sum_{k=1}^K \phi_k = 1$, $\sum_{k=1}^K \phi_{k'k} = 1$. In the ACE researches based on HMMs, the transition probability matrices typically have high self-transition probability, which reflects the continuity of chord label sequences [16]. In this paper, we set $\phi_{kk} = 0.9$. The effects of (3) and (4) are compared in Section IV-B.

Since we have no strong belief about the abstract latent features \mathbf{Z} , the prior $p(\mathbf{Z})$ is set to a standard Gaussian distribution as follows:

$$p(\mathbf{Z}) = \prod_{n=1}^N \mathcal{N}(\mathbf{z}_n | \mathbf{0}_L, \mathbf{I}_L), \quad (5)$$

where $\mathbf{0}_L$ is the all-zero vector of size L and \mathbf{I}_L is the identity matrix of size $L \times L$.

C. Classification and Recognition Models

Given chroma vectors \mathbf{X} as observed data, we aim to infer the chord labels \mathbf{S} and the latent features \mathbf{Z} from \mathbf{X} and estimate the model parameters θ and ϕ in the maximum-likelihood framework. Because the DNN-based formulation makes the posterior distribution $p_{\theta, \phi}(\mathbf{S}, \mathbf{Z}|\mathbf{X}) \propto p_{\theta, \phi}(\mathbf{X}, \mathbf{S}, \mathbf{Z})$ analytically intractable, we compute it approximately with an AVI technique. More specifically, we introduce a sufficiently-expressive variational distribution $q_{\alpha, \beta}(\mathbf{S}, \mathbf{Z}|\mathbf{X})$ parametrized by α and β and optimize it such that the Kullback-Leibler (KL) divergence from $q_{\alpha, \beta}(\mathbf{S}, \mathbf{Z}|\mathbf{X})$ to $p_{\theta, \phi}(\mathbf{S}, \mathbf{Z}|\mathbf{X})$ is minimized. Considering that both \mathbf{S} and \mathbf{Z} make an effect on the generative model $p_{\theta}(\mathbf{X}|\mathbf{S}, \mathbf{Z})$, they are assumed to be conditionally independent in the inference model $q_{\alpha, \beta}(\mathbf{S}, \mathbf{Z}|\mathbf{X})$ as follows:

$$q_{\alpha, \beta}(\mathbf{S}, \mathbf{Z}|\mathbf{X}) = q_{\alpha}(\mathbf{S}|\mathbf{X})q_{\beta}(\mathbf{Z}|\mathbf{X}), \quad (6)$$

where $q_{\alpha}(\mathbf{S}|\mathbf{X})$ and $q_{\beta}(\mathbf{Z}|\mathbf{X})$ are *classification* and *recognition* models that infer \mathbf{S} and \mathbf{Z} , respectively. In our study, (6) was found to work better than $q_{\alpha, \beta}(\mathbf{S}, \mathbf{Z}|\mathbf{X}) = q_{\alpha}(\mathbf{S}|\mathbf{X})q_{\beta}(\mathbf{Z}|\mathbf{X}, \mathbf{S})$ respecting the chain rule of probability as in [32]. In this paper, these models are implemented with DNNs parameterized by α and β as follows:

$$q_{\alpha}(\mathbf{S}|\mathbf{X}) = \prod_{n=1}^N \text{Categorical}(\mathbf{s}_n | [\boldsymbol{\pi}_{\alpha}(\mathbf{X})]_n), \quad (7)$$

$$q_{\beta}(\mathbf{Z}|\mathbf{X}) = \prod_{n=1}^N \mathcal{N}(\mathbf{z}_n | [\boldsymbol{\mu}_{\beta}(\mathbf{X})]_n, [\boldsymbol{\sigma}_{\beta}^2(\mathbf{X})]_n), \quad (8)$$

where $\boldsymbol{\pi}_{\alpha}(\mathbf{X})$ is the NK -dimensional output of the DNN with parameters α , and $\boldsymbol{\mu}_{\beta}(\mathbf{X})$ and $\boldsymbol{\sigma}_{\beta}^2(\mathbf{X})$ are the NL -dimensional outputs of the DNN with parameters β . Similar to the deep generative model, the outputs of the DNNs represent the parameters of probabilistic distributions.

D. Unsupervised Learning with Non-Annotated Data

Instead of directly maximizing the log-marginal likelihood $\log p_{\theta, \phi}(\mathbf{X})$ with respect to the model parameters θ and ϕ , we maximize its variational lower bound $\mathcal{L}_{\mathbf{X}}(\theta, \phi, \alpha, \beta)$ derived by introducing $q_{\alpha, \beta}(\mathbf{S}, \mathbf{Z}|\mathbf{X})$ as follows:

$$\log p_{\theta, \phi}(\mathbf{X}) = \log \iint p_{\theta, \phi}(\mathbf{X}, \mathbf{S}, \mathbf{Z}) d\mathbf{S} d\mathbf{Z}$$

$$\begin{aligned}
&= \log \iint \frac{q_{\alpha,\beta}(\mathbf{S}, \mathbf{Z}|\mathbf{X})}{q_{\alpha,\beta}(\mathbf{S}, \mathbf{Z}|\mathbf{X})} p_{\theta,\phi}(\mathbf{X}, \mathbf{S}, \mathbf{Z}) d\mathbf{S}d\mathbf{Z} \\
&\geq \iint q_{\alpha,\beta}(\mathbf{S}, \mathbf{Z}|\mathbf{X}) \log \frac{p_{\theta,\phi}(\mathbf{X}, \mathbf{S}, \mathbf{Z})}{q_{\alpha,\beta}(\mathbf{S}, \mathbf{Z}|\mathbf{X})} d\mathbf{S}d\mathbf{Z} \\
&\triangleq \mathcal{L}_{\mathbf{X}}(\theta, \phi, \alpha, \beta), \tag{9}
\end{aligned}$$

where the equality holds, *i.e.*, $\mathcal{L}_{\mathbf{X}}(\theta, \phi, \alpha, \beta)$ is maximized, if and only if $q_{\alpha,\beta}(\mathbf{S}, \mathbf{Z}|\mathbf{X}) = p_{\theta,\phi}(\mathbf{S}, \mathbf{Z}|\mathbf{X})$. Note that this condition cannot be satisfied because $p_{\theta,\phi}(\mathbf{S}, \mathbf{Z}|\mathbf{X})$ is hard to compute. Because the gap between $\log p_{\theta,\phi}(\mathbf{X})$ and $\mathcal{L}_{\mathbf{X}}(\theta, \phi, \alpha, \beta)$ in (9) is equal to the KL divergence from $q_{\alpha,\beta}(\mathbf{S}, \mathbf{Z}|\mathbf{X})$ to $p_{\theta,\phi}(\mathbf{S}, \mathbf{Z}|\mathbf{X})$, the minimization of the KL divergence is equivalent to the maximization of $\mathcal{L}_{\mathbf{X}}(\theta, \phi, \alpha, \beta)$.

To approximately compute $\mathcal{L}_{\mathbf{X}}(\theta, \phi, \alpha, \beta)$, we use Monte Carlo integration as follows:

$$\begin{aligned}
&\mathcal{L}_{\mathbf{X}}(\theta, \phi, \alpha, \beta) \\
&= \mathbb{E}_{q_{\alpha}(\mathbf{S}|\mathbf{X})q_{\beta}(\mathbf{Z}|\mathbf{X})}[\log p_{\theta}(\mathbf{X}|\mathbf{S}, \mathbf{Z})] \\
&\quad + \mathbb{E}_{q_{\alpha}(\mathbf{S}|\mathbf{X})q_{\beta}(\mathbf{Z}|\mathbf{X})}[\log p(\mathbf{Z}) - \log q_{\beta}(\mathbf{Z}|\mathbf{X})] \\
&\quad + \mathbb{E}_{q_{\alpha}(\mathbf{S}|\mathbf{X})}[\log p_{\phi}(\mathbf{S}) - \log q_{\alpha}(\mathbf{S}|\mathbf{X})] \\
&\approx \frac{1}{I} \sum_{i=1}^I \log p_{\theta}(\mathbf{X}|\mathbf{S}_i, \mathbf{Z}_i) - \text{KL}(q_{\beta}(\mathbf{Z}|\mathbf{X})||p(\mathbf{Z})) \\
&\quad + \text{Entropy}[q_{\alpha}(\mathbf{S}|\mathbf{X})] + \mathbb{E}_{q_{\alpha}(\mathbf{S}|\mathbf{X})}[\log p_{\phi}(\mathbf{S})], \tag{10}
\end{aligned}$$

where $\{\mathbf{S}_i, \mathbf{Z}_i\}_{i=1}^I$ are I samples drawn from $q_{\alpha}(\mathbf{S}|\mathbf{X})q_{\beta}(\mathbf{Z}|\mathbf{X})$. Following the typical VAE implementation, we set $I = 1$ and hence the index i can be omitted. To make (10) partially differentiable with respect to the model parameters θ, ϕ, α , and β , we use reparametrization tricks [8], [38] for deterministically representing the categorical variables \mathbf{S} and the Gaussian variables \mathbf{Z} as follows:

$$\epsilon_n^{\mathbf{s}} \sim \text{Gumbel}(\mathbf{0}_K, \mathbf{1}_K), \tag{11}$$

$$\mathbf{s}_n = \text{softmax}((\log[\boldsymbol{\pi}_{\alpha}(\mathbf{X})]_n + \epsilon_n^{\mathbf{s}})/\tau), \tag{12}$$

$$\epsilon_n^{\mathbf{z}} \sim \mathcal{N}(\mathbf{0}_L, \mathbf{I}_L), \tag{13}$$

$$\mathbf{z}_n = [\boldsymbol{\mu}_{\beta}(\mathbf{X})]_n + \epsilon_n^{\mathbf{z}} \odot [\boldsymbol{\sigma}_{\beta}(\mathbf{X})]_n, \tag{14}$$

where (11) indicates the standard Gumbel distribution, $\mathbf{1}_K$ is the all-one vector of size K , \odot means the element-wise product, and $\tau > 0$ is a temperature parameter that controls the uniformity of \mathbf{s}_n ($\tau = 0.1$ in this paper).

We can now compute the four terms of (10) evaluating the fitness of \mathbf{S} and \mathbf{Z} : a reconstruction term indicating the likelihood of \mathbf{S} and \mathbf{Z} for \mathbf{X} and three regularization terms making the posterior $q_{\beta}(\mathbf{Z}|\mathbf{X})$ close to the prior $p(\mathbf{Z})$, increasing the entropy of $q_{\alpha}(\mathbf{S}|\mathbf{X})$, and making \mathbf{S} temporally coherent, respectively (Fig. 2). More specifically, the first term is given by (2) and the second and third terms are given by

$$\begin{aligned}
&\text{KL}(q_{\beta}(\mathbf{Z}|\mathbf{X})||p(\mathbf{Z})) \\
&= \sum_{n=1}^N \sum_{k=1}^K \left(\frac{([\boldsymbol{\sigma}_{\beta}(\mathbf{X})]_{nk}^2 + [\boldsymbol{\mu}_{\beta}(\mathbf{X})]_{nk}^2 - 1}{2} - \log([\boldsymbol{\sigma}_{\beta}(\mathbf{X})]_{nk})) \right), \tag{15}
\end{aligned}$$

$$\begin{aligned}
&\text{Entropy}[q_{\alpha}(\mathbf{S}|\mathbf{X})] \\
&= - \sum_{n=1}^N \sum_{k=1}^K [\boldsymbol{\pi}_{\alpha}(\mathbf{X})]_{nk} \log([\boldsymbol{\pi}_{\alpha}(\mathbf{X})]_{nk}). \tag{16}
\end{aligned}$$

The last term $\mathbb{E}_{q_{\alpha}(\mathbf{S}|\mathbf{X})}[\log p_{\theta}(\mathbf{S})]$ can be calculated analytically. If $p_{\theta}(\mathbf{S})$ is the uniform distribution given by (3), we have

$$\mathbb{E}_{q_{\alpha}(\mathbf{S}|\mathbf{X})}[\log p(\mathbf{S})] = - \sum_{n=1}^N \sum_{k=1}^K [\boldsymbol{\pi}_{\alpha}(\mathbf{X})]_{nk} \log K. \tag{17}$$

If $p_{\theta}(\mathbf{S})$ is the Markov model given by (4), we use a dynamic programming technique similar to the forward algorithm of the HMM. Let $\gamma(\mathbf{s}_n) = \mathbb{E}_{q_{\alpha}(\mathbf{S}|\mathbf{X})}[\log p(\mathbf{s}_{1:n})]$ be a forward message at frame n , which can be calculated recursively as follows:

$$\gamma(\mathbf{s}_1) = \log p(\mathbf{s}_1), \tag{18}$$

$$\gamma(\mathbf{s}_n) = \sum_{\mathbf{s}_{n-1}} q_{\alpha}(\mathbf{s}_{n-1}|\mathbf{X}) (\gamma(\mathbf{s}_{n-1}) + \log p_{\phi}(\mathbf{s}_n|\mathbf{s}_{n-1})), \tag{19}$$

$$\mathbb{E}_{q_{\alpha}(\mathbf{S}|\mathbf{X})}[\log p_{\phi}(\mathbf{S})] = \sum_{\mathbf{s}_N} q_{\alpha}(\mathbf{s}_N|\mathbf{X}) \gamma(\mathbf{s}_N). \tag{20}$$

We now have a VAE (Fig. 2) that consists of:

- the deep classification model $q_{\alpha}(\mathbf{S}|\mathbf{X})$ given by (7) with the reparametrization trick given by (11) and (12),
- the deep recognition model $q_{\beta}(\mathbf{Z}|\mathbf{X})$ given by (8) with the reparametrization trick given by (13) and (14), and
- the deep generative model $p_{\theta}(\mathbf{X}|\mathbf{S}, \mathbf{Z})$ given by (2) with the prior distributions $p_{\phi}(\mathbf{S})$ and $p(\mathbf{Z})$ given by (4) and (5), respectively.

In the unsupervised condition, all models are jointly optimized in the framework of the VAE by using a variant of stochastic gradient descent such that (10) is maximized with respect to θ, α , and β .

E. Supervised Learning with Annotated Data

Under the supervised condition that chroma vectors \mathbf{X} and the corresponding chord labels \mathbf{S} are given as observed data, we aim to maximize a variational lower bound $\mathcal{L}_{\mathbf{X},\mathbf{S}}(\theta, \beta)$ of the log-likelihood $\log p_{\theta}(\mathbf{S}|\mathbf{X})$, which can be derived in a way similar to (9) as follows:

$$\begin{aligned}
\log p_{\theta}(\mathbf{X}|\mathbf{S}) &= \log \int \frac{q_{\beta}(\mathbf{Z}|\mathbf{X})}{q_{\beta}(\mathbf{Z}|\mathbf{X})} p_{\theta}(\mathbf{X}|\mathbf{Z}, \mathbf{S}) d\mathbf{Z} \\
&\geq \int q_{\beta}(\mathbf{Z}|\mathbf{X}) \log \frac{p_{\theta}(\mathbf{X}|\mathbf{Z}, \mathbf{S})}{q_{\beta}(\mathbf{Z}|\mathbf{X})} d\mathbf{Z} \\
&\triangleq \mathcal{L}_{\mathbf{X},\mathbf{S}}(\theta, \beta). \tag{21}
\end{aligned}$$

Using Monte Carlo integration, $\mathcal{L}_{\mathbf{X},\mathbf{S}}(\theta, \beta)$ can be approximately computed as follows:

$$\begin{aligned}
&\mathcal{L}_{\mathbf{X},\mathbf{S}}(\theta, \beta) \\
&\triangleq \mathbb{E}_{q_{\beta}(\mathbf{Z}|\mathbf{X})}(\log p_{\theta}(\mathbf{X}|\mathbf{S}, \mathbf{Z}) + \log p(\mathbf{Z}) - \log q_{\beta}(\mathbf{Z}|\mathbf{X})) \\
&\approx \frac{1}{I} \sum_{i=1}^I \log p_{\theta}(\mathbf{X}|\mathbf{S}_i, \mathbf{Z}_i) + \text{KL}(q_{\beta}(\mathbf{Z}|\mathbf{X})||p(\mathbf{Z})), \tag{22}
\end{aligned}$$

where $\{\mathbf{Z}_i\}_{i=1}^I$ are I samples drawn from $q_{\beta}(\mathbf{Z}|\mathbf{X}, \mathbf{S})$ using the reparametrization trick ($I = 1$ in this paper). Because the chord estimator $q_{\alpha}(\mathbf{S}|\mathbf{X})$, which plays a central role in ACE, does not appear in (22), $q_{\alpha}(\mathbf{S}|\mathbf{X})$ cannot be trained only by

maximizing (22). As suggested in the semi-supervised learning of a VAE [32], one could thus define an alternative objective function $\mathcal{L}_{\mathbf{X},\mathbf{S}}(\theta, \alpha, \beta)$ including α by adding a classification performance term to (22) as follows:

$$\mathcal{L}_{\mathbf{X},\mathbf{S}}(\theta, \alpha, \beta) \triangleq \mathcal{L}_{\mathbf{X},\mathbf{S}}(\theta, \beta) + \log q_{\alpha}(\mathbf{S}|\mathbf{X}). \quad (23)$$

A problem of this approach, however, is that the regularization terms (16) and (20) enhancing the entropy of $q_{\alpha}(\mathbf{S}|\mathbf{X})$ (preventing the overfitting) and smoothing the output of $q_{\alpha}(\mathbf{S}|\mathbf{X})$, respectively, are not taken into account.

To solve this problem, we propose a new objective function $\mathcal{L}_{\mathbf{X},\mathbf{S}}(\theta, \phi, \alpha, \beta)$ by summing (10) and (23) as follows:

$$\mathcal{L}_{\mathbf{X},\mathbf{S}}(\theta, \phi, \alpha, \beta) = \mathcal{L}_{\mathbf{X}}(\theta, \phi, \alpha, \beta) + \mathcal{L}_{\mathbf{X},\mathbf{S}}(\theta, \alpha, \beta). \quad (24)$$

In this function, the chroma vectors \mathbf{X} with the annotations \mathbf{S} are used twice as unsupervised and supervised training data as if they were *not* annotated (first term) and as they are (second term), respectively.

F. Semi-supervised Learning

Under the semi-supervised condition that partially-annotated chroma vectors are available, we define an objective function by summing the objective functions (10) and (24) corresponding to the unsupervised and supervised conditions, respectively, as follows:

$$\begin{aligned} \mathcal{L}'_{\mathbf{X},\mathbf{S}}(\theta, \phi, \alpha, \beta) & \\ & \triangleq \sum_{\mathbf{X} \text{ w/o } \mathbf{S}} \mathcal{L}_{\mathbf{X}}(\theta, \phi, \alpha, \beta) + \sum_{\mathbf{X} \text{ with } \mathbf{S}} \mathcal{L}_{\mathbf{X},\mathbf{S}}(\theta, \phi, \alpha, \beta), \\ & = \sum_{\mathbf{X}} \mathcal{L}_{\mathbf{X}}(\theta, \phi, \alpha, \beta) + \sum_{\mathbf{X} \text{ with } \mathbf{S}} \mathcal{L}_{\mathbf{X},\mathbf{S}}(\theta, \alpha, \beta). \end{aligned} \quad (25)$$

Note that $q_{\alpha}(\mathbf{S}|\mathbf{X})$ can always be regularized by $p_{\theta}(\mathbf{X}|\mathbf{S}, \mathbf{Z})$ and $p_{\phi}(\mathbf{S})$ regardless of the availability of annotations.

G. Training and Prediction

The model parameters θ , ϕ , α , and β can be optimized with a stochastic gradient descent method (e.g., Adam [39]) such that the objective function (10), (24), or (25) is maximized. Nonetheless, in this paper, ϕ is fixed (not optimized) because of its wide acceptable range (see Section IV-B3). Under the semi-supervised condition, each mini-batch consists of non-annotated and annotated chroma vectors (50%–50% in this paper) randomly selected from the training dataset.

In the test phase, using the neural chord estimator $q_{\alpha}(\mathbf{S}|\mathbf{X})$, a sequence of the posterior probabilities of chord labels \mathbf{S} are calculated from a sequence of chroma vectors \mathbf{X} extracted from a target music signal. The optimal temporally-coherent path of chord labels is then estimated via the Viterbi algorithm with the transition probabilities ϕ .

IV. EVALUATION

This section reports comparative experiments conducted for evaluating the effectiveness of the proposed method. Specifically, we investigate the effectiveness of the VAE-based regularized training, that of using the Markov prior on chord labels, and, that of using external non-annotated data.

TABLE I
EXPERIMENTAL CONDITIONS

	Training	Regularization	Prior
ACE-SL (baseline)	Supervised	NA	NA
VAE-UN-SL	Supervised	VAE-based	Uniform
VAE-MR-SL	Supervised	VAE-based	Markov
VAE-UN-SSL	Semi-supervised	VAE-based	Uniform
VAE-MR-SSL	Semi-supervised	VAE-based	Markov

TABLE II
DURATIONS OF CHORD TYPES IN DATASETS USED FOR EVALUATION

Chord type	Duration [h]
maj	53.09
min	16.63
aug	0.15
dim	0.36
sus4	1.63
sus2	0.25
1	0.76
5	0.84

A. Experimental Conditions

We here explain compared ACE methods, network configurations, datasets, and evaluation procedures and measures.

1) *Compared Methods*: As listed in Table I, we trained a chord estimator $q_{\alpha}(\mathbf{S}|\mathbf{X})$ in five different ways:

- **ACE-SL (baseline)**: As in most ACE methods, $q_{\alpha}(\mathbf{S}|\mathbf{X})$ was trained in a *supervised* manner by minimizing the cross-entropy loss for the ground-truth labels \mathbf{S} , i.e., maximizing the following objective function:

$$\mathcal{L}_{\mathbf{X},\mathbf{S}}(\alpha) = \log q_{\alpha}(\mathbf{S}|\mathbf{X}). \quad (26)$$

- **VAE-UN-SL**: $q_{\alpha}(\mathbf{S}|\mathbf{X})$ was trained in a *supervised* manner by maximizing (24) with the uniform prior (3).
- **VAE-MR-SL**: $q_{\alpha}(\mathbf{S}|\mathbf{X})$ was trained in a *supervised* manner by maximizing (24) with the Markov prior (4).
- **VAE-UN-SSL**: $q_{\alpha}(\mathbf{S}|\mathbf{X})$ was trained in a *semi-supervised* manner by maximizing (25) with the uniform prior (3).
- **VAE-MR-SSL**: $q_{\alpha}(\mathbf{S}|\mathbf{X})$ was trained in a *semi-supervised* manner by maximizing (25) with the Markov prior (4).

For convenience, let ‘*’ denote the wild-card character, e.g., **VAE-*-SL** means **VAE-MR-SL** or **VAE-UN-SL**.

Comparing **ACE-SL** with **VAE-*-SL**, we evaluated the effectiveness of the VAE architecture in regularizing $q_{\alpha}(\mathbf{S}|\mathbf{X})$. Comparing **VAE-*-SSL** with **VAE-*-SL**, we evaluated the effectiveness of the semi-supervised learning. Comparing **VAE-MR-*** with **VAE-UN-***, we evaluated the effectiveness of the Markov prior on \mathbf{S} .

2) *Network Configurations*: Each of the classifier $q_{\alpha}(\mathbf{S}|\mathbf{X})$, the recognizer $q_{\beta}(\mathbf{Z}|\mathbf{X})$, and the generator $p_{\theta}(\mathbf{X}|\mathbf{S}, \mathbf{Z})$ was implemented with a three-layered BLSTM network [40] followed by layer normalization [41]. The final layer of $q_{\alpha}(\mathbf{S}|\mathbf{X})$ consisted of softmax functions that output the frame-level posterior probabilities of K chord labels. The final layer of $q_{\beta}(\mathbf{Z}|\mathbf{X})$ consisted of linear units that output $\mu_{\beta}(\mathbf{X})$ and $\log \sigma_{\beta}^2(\mathbf{X})$. The final layer of $p_{\theta}(\mathbf{X}|\mathbf{S}, \mathbf{Z})$ consisted of sigmoid functions that output $\omega_{\theta}(\mathbf{S}, \mathbf{Z})$. Each hidden layer of the BLSTM had 256 units. Because the architecture of $q_{\alpha}(\mathbf{S}|\mathbf{X})$ was similar to that of a state-of-the-art chord estimator [36], ACE-SL was considered to be a reasonable baseline method.

We used Adam optimizer [39], where the learning rate was first set to 0.001 and then decreased exponentially by a scaling factor of 0.99 per epoch. Gradient clipping with norm 5 was additionally applied to the optimization process. Each mini-batch consisted of 16 sequences, each of which contained 645 frames (1 min). The parameter of the Markov prior ϕ was fixed as stated in III-B, and θ , α and β were iteratively updated. In all the methods and configurations, the number of training epochs was set to 300, which was sufficiently large to reach convergence (early stopping was not used).

3) *Datasets*: We collected 1210 *annotated* popular songs consisting of 198 songs from Isophonics [37], 100 songs from RWC-MDB-P-2001 [42], 186 songs from uspop2002 [43]², and 726 songs from McGill Billboard dataset [44]. As shown in Table II, the six types of triad chords and the two types of power chords are heavily imbalanced in the chord annotations, where most of the annotated chord labels belong to the *major* and *minor* triads. We also collected 700 *non-annotated* popular songs composed by Japanese and American artists.

Each music signal sampled at 44.1kHz was analyzed with constant-Q transform (CQT) with a shifting interval of 4096 points and a frequency resolution of one semitone per bin. The CQT spectrogram and its 1-, 2-, 3-, and 4-octave-shifted versions were stacked to yield a five-layered harmonic CQT (HCQT) representation, which was fed to a neural multi-pitch estimator [36] for computing chroma vectors \mathbf{X} . To compensate for the imbalance of the ratios of the 12 chord roots in the training data, chroma vectors and chord labels were jointly pitch-rotated by a random number of semitones on each training iteration. Pitch shifting of the multi-channel chroma vectors can be done by performing vector rotation on each channel, and pitch shifting of chord annotations can be done by changing the root notes.

4) *Evaluation Procedures*: To conduct five-fold cross validation, we divided the 1210 annotated songs into five subsets (242 songs each). In each fold, one of the subsets was kept as test data and the remaining four subsets were used as training data, in which I and $4-I$ subsets were treated as annotated and non-annotated songs, respectively ($I \in \{1, 2, 3, 4\}$). Not only the classifier $q_\alpha(\mathbf{S}|\mathbf{X})$ but also the recognizer $q_\beta(\mathbf{Z}|\mathbf{X})$ and the generator $p_\theta(\mathbf{X}|\mathbf{S}, \mathbf{Z})$ were trained jointly by using all the training data (VAE-*-SSL) or only the annotated data (VAE-*-SL). In ACE-SL, in contrast, only the classifier $q_\alpha(\mathbf{S}|\mathbf{X})$ was trained by using the annotated data.

VAE-*-SSL was additionally tested under *extended* semi-supervised conditions that annotated 976 songs (four subsets) and M non-annotated songs ($M \in \{250, 500, 700\}$) were used as training data in each fold. Note that the performance was measured on the remaining 242 annotated songs, which did not overlap with the 700 non-annotated songs.

5) *Evaluation Measures*: The chord estimation performance (accuracy) of each method was measured in terms of the frame-level match rate between the estimated and ground-truth chord sequences. The weighed accuracy for each song was measured with *mir_eval* library [45] in terms of the *majmin* criterion

considering only the *major* and *minor* triads plus the *no-chord* label ($K = 25$) and the *triads* criterion with the vocabulary defined in Section III-A ($K = 97$). The overall accuracy was given as the average of the song-wise accuracies weighed by the song lengths.

B. Experimental Results

The overall accuracies of ACE-SL and VAE-*-* with respect to the numbers of annotated and non-annotated songs (denoted as $A+B$) used for training are shown in Fig. 3. To investigate the temporal continuity of \mathbf{S} induced by the Markov prior, we tested VAE-MR-SSL with a self-transition probability $\phi_{kk} \in \{1/K, 0.3, 0.5, 0.7, 0.9\}$. The song-wise accuracies and average chord durations at 976+0 and 976+700 are compared in Fig. 4. Examples of estimated chord sequences estimated by ACE-SL, VAE-UN-SSL, and VAE-MR-SSL with $\phi_{kk} = 0.9$ are shown in Fig. 5.

1) *Evaluation of VAE-Based Regularized Training*: We confirmed the effectiveness of the VAE-based regularized training of $q_\alpha(\mathbf{S}|\mathbf{X})$ under all the conditions. As shown in Fig. 3 and Fig. 4(a), VAE-*-SL clearly outperformed ACE-SL by a large margin around 1 pts. $q_\alpha(\mathbf{S}|\mathbf{X})$ was regularized effectively by considering its entropy, the Markov or uniform prior of \mathbf{S} , and the reconstruction of \mathbf{X} based on \mathbf{S} and \mathbf{Z} .

2) *Evaluation of Semi-supervised Learning*: We confirmed the effectiveness of the semi-supervised learning of $q_\alpha(\mathbf{S}|\mathbf{X})$. Under the semi-supervised conditions at 244+732, 488+488, and 732+244 in the left half of Fig. 3, VAE-MR-SSL and VAE-UN-SSL outperformed VAE-MR-SL and VAE-UN-SL, respectively, where the proposed VAE-MR-SSL worked best. The success of the semi-supervised learning was attributed to the fact that the musical and acoustic characteristics of the 976 songs used for training were consistent with those of the 244 songs used for testing in the five-fold cross validation with the 1210 songs. Under the supervised condition at 976+0, VAE-MR-SSL and VAE-UN-SSL were equivalent to VAE-MR-SL and VAE-UN-SL, respectively.

Under the *extended* semi-supervised conditions at 976+250, 976+500, and 976+700 in the right half of Fig. 3, the performance once dropped and then barely recovered according to the increase of non-annotated songs used for training. The large difference in the musical and acoustic characteristics of the annotated and non-annotated songs is considered to have hindered the semi-supervised learning.

3) *Evaluation of Markov Prior*: We confirmed the effectiveness of the Markov prior on \mathbf{S} under all the conditions. Under the semi-supervised conditions at 244+732, 488+488, and 732+244 and the supervised condition at 976+0 in the left half of Fig. 3, VAE-MR-SL and VAE-MR-SSL outperformed VAE-UN-SL and VAE-UN-SSL, respectively. The Markov prior played a vital role under the *extended* semi-supervised conditions at 976+250, 976+500, and 976+700 in the right half of Fig. 3. While VAE-UN-SSL at 976+250 significantly underperformed VAE-UN-SSL at 976+0, VAE-MR-SSL did not experience large performance drop and achieved slightly better performance at 976+700 by encouraging $q_\alpha(\mathbf{S}|\mathbf{X})$ to yield a temporally-smooth estimate of \mathbf{S} .

² The annotations for RWC-MDB-P-2001 and uspop2002 are provided by the Music and Audio Research Lab at NYU.

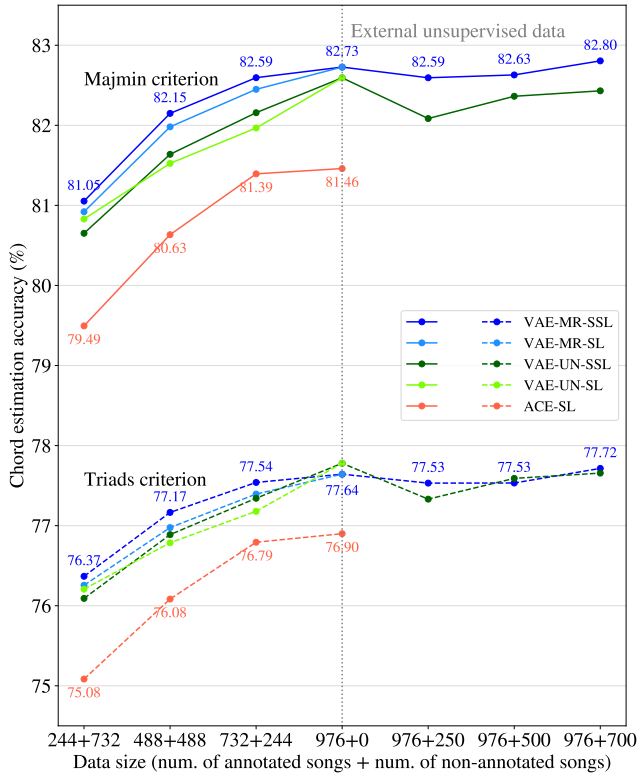


Fig. 3. The experimental results of the five-fold cross validation using the 1210 annotated songs and the 700 external non-annotated songs.

Fig. 4(b) shows that the Markov prior mitigated the negative effect of the semi-supervised learning. **VAE-MR-SSL** with $\phi_{kk} = 1/K$ performed better, but yielded finer chord segments than **ACE-SL** because $q_{\alpha}(\mathbf{S}|\mathbf{X})$ was trained under a condition that chord labels were allowed to change frequently for non-annotated songs such that the unsupervised learning objective (10) was maximized. In contrast, **VAE-MR-SSL** with a higher self-transition probability yielded longer chord segments and the chord durations were distributed in a way similar to the ground-truth data. As shown in Fig. 4(a), the choice of the self-transition probability between 0.3 and 0.9 had a small impact on the overall chord estimation accuracies.

In Fig. 5, some errors made by **ACE-SL** (light-green segments) were corrected by the VAE-based methods. The chord label sequence obtained by **VAE-UN-SSL**, however, included a number of incorrect short fragments caused by the local fluctuations of the chroma vectors. As discussed above, $q_{\alpha}(\mathbf{S}|\mathbf{X})$ was encouraged to frequently vary over time such that the fine structure of chroma vectors could be reconstructed precisely in the VAE framework. In contrast, the chord label sequence obtained by **VAE-MR-SSL** included fewer transitions and was much closer to the ground-truth sequence.

C. Further Observations

Fig. 6 shows the confusion matrices obtained by **ACE-SL** and **VAE-MR-SSL**. While the accuracies on the *maj*, *min*, *aug* and *dim* types were improved by **VAE-MR-SSL**, the accuracies on the other uncommon chord types were significantly degraded. Rare chords tended to be wrongly classified to the

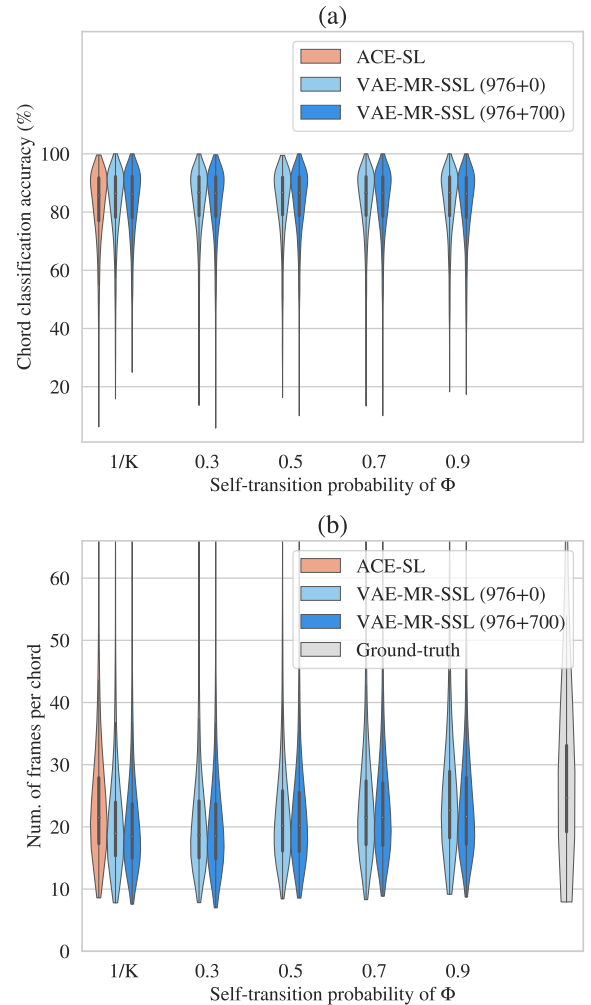


Fig. 4. The song-wise accuracies (in *majmin* criterion) and average durations of chord labels estimated by **ACE-SL** and **VAE-MR-SSL** with different self-transition probabilities ($\phi_{kk} \in \{1/K, 0.3, 0.5, 0.7, 0.9\}$), where **VAE-MR-SSL** with $\phi_{kk} = 1/K$ is equivalent to **VAE-UN-SSL**. The chord durations were measured before the Viterbi post-filtering.

maj and *min* triads. Interestingly, the accuracies on the eight chord types were not necessarily correlated to their ratios in the training data (Table II), where the *sus4* triads were much more frequently used than the *aug* and *dim* triads. The same problem occurred in **VAE-UN-SSL** because the unsupervised learning objective (10) has no mechanism to prevent $q_{\alpha}(\mathbf{S}|\mathbf{X})$ from excessively yielding popular chord types.

As shown in Fig. 7, the generative model $p_{\theta}(\mathbf{X}|\mathbf{S}, \mathbf{Z})$ successfully reconstructed chroma vectors, conditioned by the *maj*, *min*, *aug*, and *dim* triads, *i.e.*, the reconstructed chroma vectors had high probabilities on the pitch classes of the chord notes. In contrast, $p_{\theta}(\mathbf{X}|\mathbf{S}, \mathbf{Z})$ failed to reconstruct chroma vectors, when conditioned by the *sus2* and *sus4* triads and the power chords. Comparing Fig. 6 with Fig. 7, we investigate the relationships between the estimation accuracy of chord labels and the reconstruction quality of chroma vectors. The generator $p_{\theta}(\mathbf{X}|\mathbf{S}, \mathbf{Z})$ failed to learn the pitch-class distributions of several chord classes (*e.g.*, *sus2* and *sus4*) whose chroma vectors often had no clear peaks on the chord notes. For such

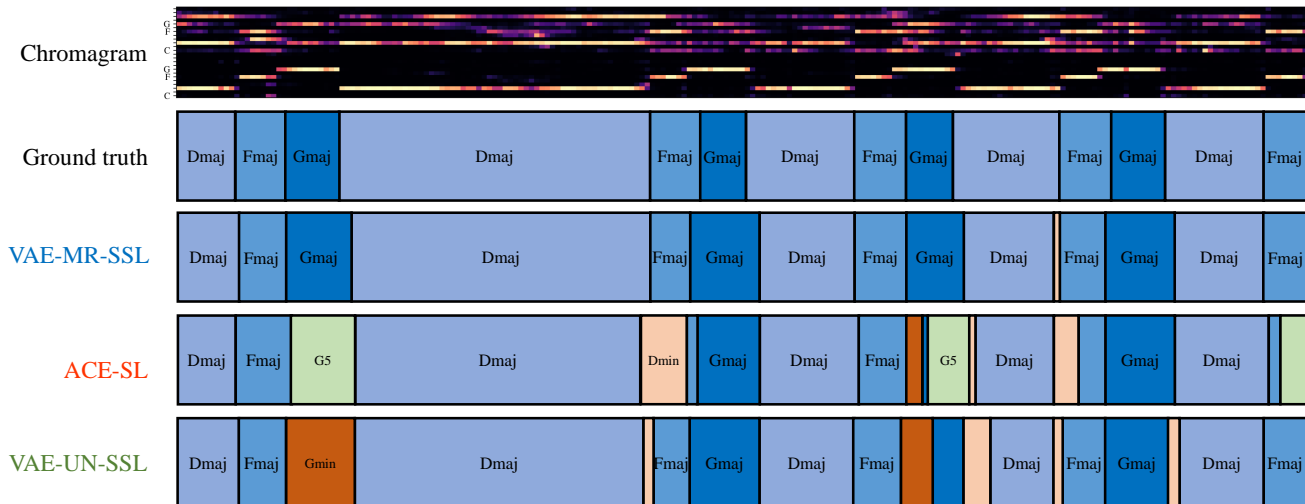


Fig. 5. An example of chord label sequences estimated by the supervised and semi-supervised methods without the Viterbi post-filtering. For readability, only the first 24 dimensions (bass and middle channels) of the chroma vectors are displayed.

chroma vectors, $p_{\theta}(\mathbf{X}|\mathbf{S}, \mathbf{Z})$ always gave a lower probability even if \mathbf{S} was the ground-truth chord classes corresponding to \mathbf{X} . Note that $p_{\theta}(\mathbf{X}|\mathbf{S}, \mathbf{Z})$ was used for regularizing the classifier $q_{\alpha}(\mathbf{S}|\mathbf{X})$ in the unsupervised learning objective (10), where $q_{\alpha}(\mathbf{S}|\mathbf{X})$ was trained to avoid *sus2* and *sus4* triads and favor *maj* triads to maximize $p_{\theta}(\mathbf{X}|\mathbf{S}, \mathbf{Z})$.

V. CONCLUSION

This paper described a statistical method that trains a neural chord estimator in a semi-supervised manner by constructing a VAE with latent chord labels and features. This is a new approach to ACE that unifies the generative and discriminative methods. Our method incorporates a Markov prior on chord labels to encourage the temporal continuity of chord labels estimated with the chord estimator. The comparative experiment clearly showed the effectiveness of using the generative model of chroma vectors and the Markov prior on chord labels in regularizing the chord estimator for performance improvement. The limitation of the proposed semi-supervised learning is that the trained chord classifier tends to mistakenly classify some specific chord types into popular types. This may become more problematic when a larger chord vocabulary including seventh chords and chord inversions is used.

The success of the semi-supervised VAE for ACE indicates the effectiveness of unifying the deep generative and discriminative methods in automatic music transcription (AMT). Using the AVI framework, we can explicitly introduce prior knowledge on musical symbol sequences as a regularization term. Such knowledge is hard to automatically extract from training data in supervised discriminative methods. One way to improve the performance of ACE is to replace the frame-level Markov prior of chord labels with a beat- or symbol-level language model, which has been considered to be effective for solving the ambiguity in acoustic features [23], [24]. We also plan to develop a comprehensive AMT system based on a unified VAE that can treat mutually-dependent musical elements such as keys, beats, and notes as latent variables.

REFERENCES

- [1] M. Goto, K. Yoshii, H. Fujihara, M. Mauch, and T. Nakano, "Songle: A web service for active music listening improved by user contributions," in *proceedings of the International Society for Music Information Retrieval (ISMIR)*, 2011, pp. 311–316.
- [2] A. Anglade, R. Ramirez, and S. Dixon, "Genre classification using harmony rules induced from automatic chord transcriptions," in *proceedings of the International Society for Music Information Retrieval (ISMIR)*, 2009, pp. 669–674.
- [3] J. P. Bello, "Audio-based cover song retrieval using approximate chord sequences: Testing shifts, gaps, swaps and beats," in *proceedings of the International Society for Music Information Retrieval (ISMIR)*, vol. 7, 2007, pp. 239–244.
- [4] J. Pauwels, K. O'Hanlon, E. Gómez, and M. B. Sandler, "20 years of automatic chord recognition from audio," in *proceedings of the International Society for Music Information Retrieval (ISMIR)*, 2019, pp. 54–63.
- [5] K. Lee and M. Slaney, "Acoustic chord transcription and key extraction from audio using key-dependent hmms trained on synthesized audio," *IEEE Transactions on Audio, Speech, and Language Processing*, vol. 16, no. 2, pp. 291–301, Feb 2008.
- [6] M. McVicar, R. Santos-Rodríguez, Y. Ni, and T. D. Bie, "Automatic chord estimation from audio: A review of the state of the art," *IEEE/ACM Transactions on Audio, Speech, and Language Processing*, vol. 22, no. 2, pp. 556–575, 2014.
- [7] E. J. Humphrey and J. P. Bello, "Four timely insights on automatic chord estimation," in *proceedings of the International Society for Music Information Retrieval*, 10 2015, pp. 673–679.
- [8] D. P. Kingma and M. Welling, "Auto-encoding variational Bayes," in *proceedings of the International Conference on Learning Representations (ICLR)*, 2014, pp. 1–14.
- [9] S. Gershman and N. Goodman, "Amortized inference in probabilistic reasoning," in *Proceedings of the annual meeting of the cognitive science society*, vol. 36, no. 36, 2014, pp. 517–522.
- [10] L. R. Rabiner, "A tutorial on hidden markov models and selected applications in speech recognition," *Proceedings of the IEEE*, vol. 77, no. 2, pp. 257–286, 1989.
- [11] T. Fujishima, "Realtime chord recognition of musical sound: A system using common lisp music," in *Proceedings of the International Computer Music Conference (ICMC)*, 1999, pp. 464–467.
- [12] A. Sheh and D. Ellis, "Chord segmentation and recognition using EM-trained hidden Markov models," in *proceedings of the International Society for Music Information Retrieval (ISMIR)*, 2003, pp. 185–191.
- [13] M. Mauch and S. Dixon, "Approximate note transcription for the improved identification of difficult chords," in *proceedings of the International Society for Music Information Retrieval (ISMIR)*, 2010, pp. 135–140.

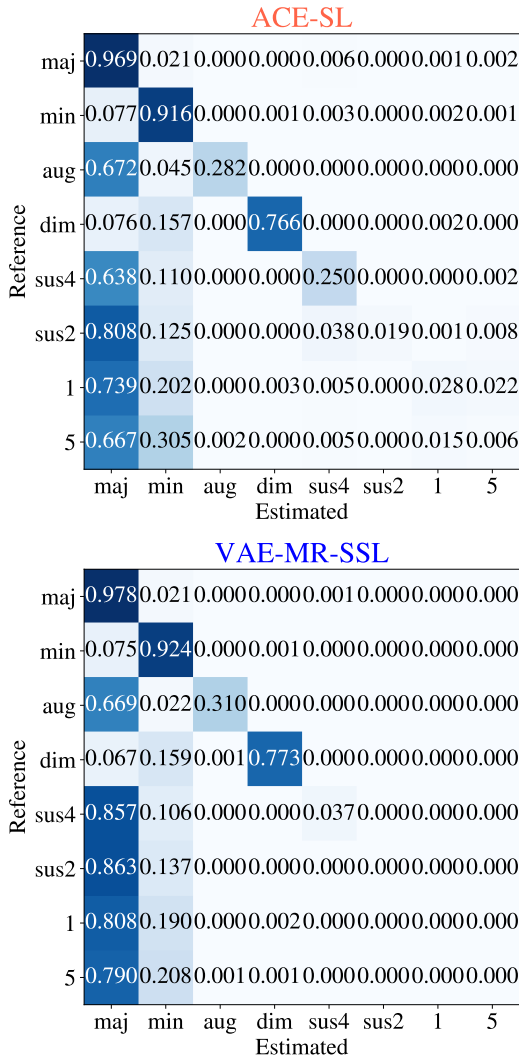


Fig. 6. Confusion matrices with respect to chord types. Estimated chords with wrong root notes are not counted.

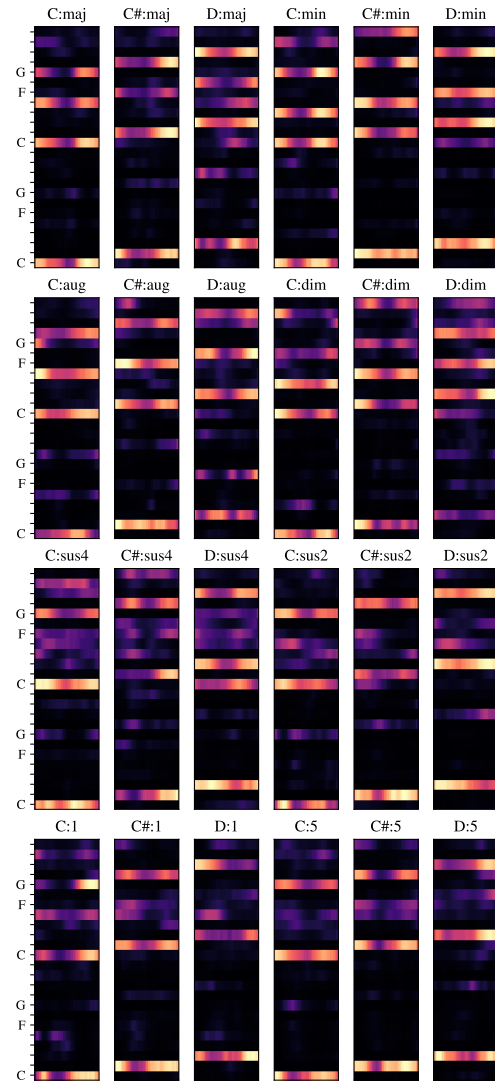


Fig. 7. The probability distributions obtained by $p_{\theta}(\mathbf{X}|\mathbf{S}, \mathbf{Z})$ conditioned by different chord labels \mathbf{S} . Only the first 24 dimensions (bass and middle channels) of the chroma vectors are displayed.

[14] Y. Ni, M. McVicar, R. Santos-Rodriguez, and T. De Bie, "An end-to-end machine learning system for harmonic analysis of music," *IEEE/ACM Transactions on Audio, Speech, and Language Processing*, vol. 20, no. 6, pp. 1771–1783, 2012.

[15] M. Khadkevich and M. Omologo, "Use of hidden markov models and factored language models for automatic chord recognition," in *proceedings of the International Society for Music Information Retrieval (ISMIR)*, 2009, pp. 561–566.

[16] R. Chen, W. Shen, A. Srinivasamurthy, and P. Chordia, "Chord recognition using duration-explicit hidden Markov models," in *proceedings of the International Society for Music Information Retrieval (ISMIR)*, 2012, pp. 445–450.

[17] E. J. Humphrey and J. P. Bello, "Rethinking automatic chord recognition with convolutional neural networks," in *2012 11th International Conference on Machine Learning and Applications*, vol. 2, 2012, pp. 357–362.

[18] C. Schörkhuber and A. Klapuri, "Constant-q transform toolbox for music processing," in *7th Sound and Music Computing Conference*, 2010.

[19] F. Korzeniewski and G. Widmer, "A fully convolutional deep auditory model for musical chord recognition," in *IEEE 26th International Workshop on Machine Learning for Signal Processing (MLSP)*, 2016, pp. 13–16.

[20] Y. Wu, T. Carsault, and K. Yoshii, "Automatic chord estimation based on a frame-wise convolutional recurrent neural network with non-aligned annotations," in *27th European Signal Processing Conference*

(*EUSIPCO*), 2019.

[21] N. Boulanger-Lewandowski, Y. Bengio, and P. Vincent, "Audio chord recognition with recurrent neural networks," in *proceedings of the International Society for Music Information Retrieval (ISMIR)*, 2013, pp. 335–340.

[22] S. Sigtia, N. Boulanger-Lewandowski, and S. Dixon, "Audio chord recognition with a hybrid recurrent neural network," in *proceedings of the International Society for Music Information Retrieval (ISMIR)*, 2015, pp. 127–133.

[23] F. Korzeniewski and G. Widmer, "On the futility of learning complex frame-level language models for chord recognition," in *AES Conference on Semantic Audio*, 2017, pp. 2–6.

[24] —, "Improved chord recognition by combining duration and harmonic language models," in *proceedings of the International Society for Music Information Retrieval (ISMIR)*, 2018, pp. 10–17.

[25] T.-P. Chen and L. Su, "Harmony transformer: Incorporating chord segmentation into harmony recognition," in *proceedings of the International Society for Music Information Retrieval (ISMIR)*, 2019, pp. 259–267.

[26] A. Vaswani, N. Shazeer, N. Parmar, J. Uszkoreit, L. Jones, A. N. Gomez, ukasz Kaiser, and I. Polosukhin, "Attention is all you need," in *Advances in Neural Information Processing Systems (NeurIPS)*, 2017, pp. 5998–6008.

[27] H. V. Koops, W. B. de Haas, J. A. Burgoyne, J. Bransen, A. Kent-Muller, and A. Volk, "Annotator subjectivity in harmony annotations of popular

- music,” *Journal of New Music Research*, vol. 48, no. 3, pp. 232–252, 2019.
- [28] B. Mcfee and J. P. Bello, “Structured training for large-vocabulary chord recognition,” in *proceedings of the International Society for Music Information Retrieval (ISMIR)*, 2017, pp. 188–194.
- [29] T. Carsault, J. Nika, and P. Esling, “Using musical relationships between chord labels in automatic chord extraction tasks,” in *proceedings of the International Society for Music Information Retrieval (ISMIR)*, 2018, pp. 18–25.
- [30] J. Jiang, K. Chen, W. Li, and G. Xia, “Large-vocabulary chord transcription via chord structure decomposition,” in *proceedings of the International Society for Music Information Retrieval (ISMIR)*, 2019, pp. 644–651.
- [31] J. Deng and Y. K. Kwok, “Large vocabulary automatic chord estimation with an even chance training scheme,” in *proceedings of the International Society for Music Information Retrieval (ISMIR)*, 2017, pp. 531–536.
- [32] D. P. Kingma, S. Mohamed, D. J. Rezende, and M. Welling, “Semi-supervised learning with deep generative models,” in *NIPS*, 2014, pp. 3581–3589.
- [33] L. Maaløe, C. K. Sønderby, S. K. Sønderby, and O. Winther, “Auxiliary deep generative models,” in *proceedings of the International Conference on Machine Learning (ICML)*, 2016, pp. 1445–1453.
- [34] T. Hori, R. F. Astudillo, T. Hayashi, Y. Zhang, S. Watanabe, and J. L. Roux, “Cycle-consistency training for end-to-end speech recognition,” in *proceedings of the International Conference on Acoustics, Speech and Signal Processing (ICASSP)*, 2019, pp. 6271–6275.
- [35] E. Dupont, “Learning disentangled joint continuous and discrete representations,” in *Advances in Neural Information Processing Systems (NeurIPS)*, 2018, pp. 710–720.
- [36] Y. Wu and W. Li, “Automatic audio chord recognition with MIDI-trained deep feature and BLSTM-CRF sequence decoding model,” *IEEE/ACM Transactions on Audio, Speech, and Language Processing*, vol. 27, no. 2, pp. 355–366, 2019.
- [37] C. Harte, “Towards automatic extraction of harmony information from music signals,” Ph.D. dissertation, Queen Mary University of London, 2010.
- [38] E. Jang, S. Gu, and B. Poole, “Categorical reparameterization with Gumbel-Softmax,” in *proceedings of the International Conference on Learning Representations (ICLR)*, 2017.
- [39] D. P. Kingma and J. Ba, “Adam: A method for stochastic optimization,” in *proceedings of the International Conference on Learning Representations (ICLR)*, 2015, pp. 1–15.
- [40] A. Graves, N. Jaitly, and A. Mohamed, “Hybrid speech recognition with deep bidirectional LSTM,” in *2013 IEEE Workshop on Automatic Speech Recognition and Understanding*, Dec 2013, pp. 273–278.
- [41] J. L. Ba, J. R. Kiros, and G. E. Hinton, “Layer normalization,” *arXiv preprint arXiv:1607.06450*, 2016.
- [42] M. Goto, H. Hashiguchi, T. Nishimura, and R. Oka, “RWC music database: Popular, classical, and jazz music databases,” in *proceedings of the International Society for Music Information Retrieval (ISMIR)*, 2002, pp. 287–288.
- [43] A. Berenzweig, B. Logan, D. Ellis, and B. Whitman, “A large-scale evaluation of acoustic and subjective music-similarity measures,” *Computer Music Journal*, vol. 28, no. 2, pp. 63–76, 2004.
- [44] J. A. Burgoyne, J. Wild, and I. Fujinaga, “An expert ground truth set for audio chord recognition and music analysis,” in *proceedings of the International Society for Music Information Retrieval (ISMIR)*, 2011, pp. 633–638.
- [45] C. Raffel, B. McFee, E. J. Humphrey, J. Salamon, O. Nieto, D. Liang, and D. P. W. Ellis, “mir_eval: A transparent implementation of common MIR metrics,” in *proceedings of the International Society for Music Information Retrieval (ISMIR)*, 2014, pp. 367–372.